

## Nuclear Interactions in Carbon Produced by Cosmic Rays with Energies between $10^{10}$ and $10^{12}$ ev\*

LUISA F. HANSEN AND W. B. FRETTER

*Department of Physics, University of California, Berkeley, California*

(Received November 16, 1959; revised manuscript received February 3, 1960)

An experiment is described in which high-energy nuclear interactions in the range of energies  $10^{10}$ – $10^{12}$  ev were analyzed by means of a cloud chamber in a magnetic field. Measurements of ionization and momentum made possible the identification of electrons and  $\pi$  mesons to about 20 Bev/c. Protons,  $K$  mesons, and hyperons could not be identified unambiguously among themselves, except in very limited regions of momentum. The primary particles were cosmic-ray nucleons and a possible fraction of pions, the target nuclei were carbon and the velocities of the primaries were determined from balance of momentum in the center-of-mass system. A total of 41 events were analyzed, and the results compared to previous experimental work and the predictions of the theories of Heisenberg and Landau. The measurements made included the transverse momenta of the secondaries and their average energy in the center-of-mass system, the energy and angular distributions of the pions and heavy particles (protons,  $K$  mesons, hyperons) in the center-of-mass system, the inelasticity of the collision, the multiplicity of the showers, the percentage of strange particles, and the positive excess of the secondaries.

### INTRODUCTION

THE nuclear interactions of cosmic rays provide information on the nature of nucleon-nucleon and pion-nucleon interactions at energies beyond those available in accelerators. Much experimental work has been done on these interactions, with nuclear emulsions and cloud chambers as detectors of the particles produced, and several theories of the interaction process have been proposed which can be compared with experiment.

Although most of the experimental data have been obtained from nuclear emulsions, there are three principal difficulties with the nuclear emulsion technique when it is applied to the analysis of these interactions. First, the emulsion is a mixture of elements, and the nature of the struck nucleus cannot readily be determined. Thus many of the observed interactions are between the incident particle and a nucleus, which may be heavy or light, rather than a single nucleon. The second difficulty is the scanning bias, which favors the detection of highly multiple events. The third problem is the difficulty of identification of the particles emerging from the interaction. Only in a limited range of energies can such identification be made.

Cloud-chamber experiments can be designed to ameliorate, if not to eliminate these difficulties, but inevitably, other problems arise. Light materials such as hydrogen,<sup>1</sup> lithium,<sup>2,3</sup> or carbon,<sup>4,5</sup> have been used to eliminate the uncertainty as to the target nucleus and to reduce the probability of successive interactions within the same nucleus. Events of low multiplicity can be detected by a cloud chamber although the

triggering efficiency usually depends on the multiplicity. Until recently the identification of particles of high energy in cloud chambers was also limited to a narrow energy range, but the experiments of Kepler et al.,<sup>6</sup> on the relativistic increase of ionization have opened a new possibility for the identification of the particles produced in high-energy nuclear interactions.

The present experiment was done with a cloud chamber in a magnetic field, and was designed to make use of the most accurate measurements possible in a cloud chamber. The target material was carbon where the probability of interaction with more than one nucleon is fairly low. Measurement of ionization and momentum of the secondary particles in the cloud chamber made possible identification of these particles up to energies of about 20 Bev. The energy of interactions observed was set by the natural energy spectrum of cosmic radiation, and is in a range of energies in which little systematic experimentation on the fundamental interactions has been possible.

### EXPERIMENTAL METHOD

#### Apparatus

The apparatus used in this experiment is shown in Fig. 1, and has been described previously.<sup>6,7</sup> The experiment was done at sea level. The cloud chamber was in a magnetic field of about 8000 gauss and was filled with a mixture of 16 cm Hg of argon and 16 cm Hg of helium, together with a mixture of ethyl alcohol and water in proportion 3:2 by volume, which produced a vapor pressure of about 4.5 cm Hg.

The nuclear interactions were produced by cosmic rays in the block of carbon above the cloud chamber. The triggering coincidence required one or more Geiger

\* Supported in part by the joint program of the Office of Naval Research and the U. S. Atomic Energy Commission.

<sup>1</sup> A. B. Weaver, Phys. Rev. **90**, 86 (1953).

<sup>2</sup> W. B. Fretter, Phys. Rev. **80**, 921 (1950).

<sup>3</sup> J. G. Askowith and K. Sitte, Phys. Rev. **97**, 159 (1955).

<sup>4</sup> J. R. Green, Phys. Rev. **80**, 832 (1950).

<sup>5</sup> N. M. Duller and W. D. Walker, Phys. Rev. **93**, 215 (1954).

<sup>6</sup> R. G. Kepler, C. A. d'Andlau, W. B. Fretter, and L. F. Hansen, Nuovo cimento **7**, 71 (1958).

<sup>7</sup> W. B. Fretter and E. W. Friesen, Rev. Sci. Instr. **26**, 703 (1955).

counters above the chamber to discharge simultaneously with three or more counters in the first tray under the chamber. The second tray under the chamber was used only to record no-field tracks of single particles traversing the chamber. The requirement of three particles below the chamber imposed a bias on the multiplicity of events observed; in spite of this, many two-particle events were observed, probably triggered by interactions in the lead above the lower tray. Most of the showers recorded were electron showers.

The minimum delay time between events was 23 minutes; 5 minutes for the cycling time of the chamber and 18 additional minutes of dead time to obtain uniform conditions for each expansion. One photograph per hour was obtained on the average, and a fully analyzable event was obtained at the rate of one in three days.

The stereoscopic camera was set at  $f/16$ , and Kodak Linagraph Ortho film was used.

**Selection of the Events**

1. Events which were clearly electron showers were rejected by visual scanning of the film.
2. Events which appeared to be nuclear in character were rejected if their origin was not within the block of carbon or if they did not fall within the fiducial lines on the back plate of the chamber.
3. Additional events were rejected if, on measurement of ionization and momentum and identification of the particles, they did not contain at least two penetrating particles. Most events containing only one penetrating particle probably originated from the knock-on or bremsstrahlung processes of  $\mu$  mesons, and our technique was not accurate enough to distinguish  $\mu$  mesons from  $\pi$  mesons. This selection process left 68 showers to be analyzed. Most of the results of this

paper are based on the analysis of 41 of these events, which contained three or more penetrating particles.

**Momentum Measurements**

The curvatures of particles with energies greater than 1 Bev were measured in an optical comparator, and the method of least squares was used to reduce the data. The usual corrections for magnification and for variation of magnetic field were made. The error in the determination of the curvature was found by making systematic measurements on no-field tracks. The maximum detectable momentum was about 30 Bev/ $c$ .

The radii of curvature of tracks of momentum less than 1 Bev/ $c$  were found by projecting the tracks to full scale and comparing them with arcs of circles of known radius.

**Ionization Measurement**

The argon-helium gas mixture was used because previous measurements<sup>6</sup> had shown that the relativistic rise of ionization in this mixture was nearly as rapid as it is in a xenon-helium mixture, and the experimental procedure with argon is much simpler than with xenon, which we had to recover on pumping out the chamber. We used the experimentally determined<sup>6</sup> ionization curve for this mixture in the measurements here described.

The ionization of the particles in the cloud chamber was measured by counting the number of droplet images along the track as viewed in a stereoscopic microscope with a magnification of 40X. In most cases the tracks were counted between the top and bottom fiducial lines, with the average length of track 46 cm. Clusters of drops (blobs) which had more than 40 drops were rejected as in previous experiments. The length of the track was measured in projection, and corrections were made for the magnification, curvature, and the number of blobs rejected. The ionization was then expressed as the number of drops per centimeter of track.

The error in the ionization measurement of an individual track was determined from a study of fifty electron showers. In such showers the identity of the particles is not in question, and the momentum of each track could be measured quite accurately. The procedure was then to calculate for each shower a hypothetical value of  $I_0$ , the ionization of a track at the minimum of the ionization curve, from the measured ionization of each electron in the shower. This gave a number of values of  $I_0$  which could be analyzed statistically to determine the standard deviation of a given ionization measurement. This error was about 5% for an individual full-length track containing about 1000 droplets.

The value of  $I_0$  for a penetrating shower picture is more difficult to determine. Ordinarily  $I_0$  does not change appreciably from one expansion to the next, so

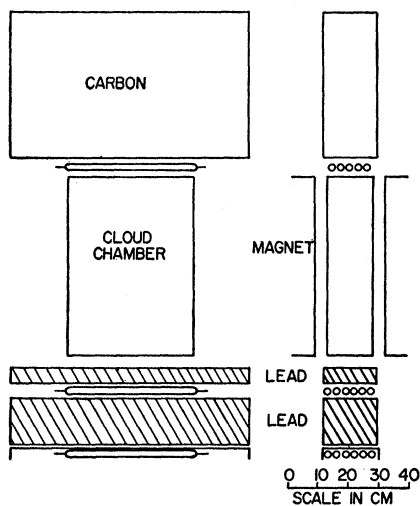


FIG. 1. The experimental apparatus.

TABLE I. Event 73309. Example of the procedure used in identification of particles. The hypothetical value of the ionization at the minimum is calculated for different particles, and a consistent set of values is sought. In this case the value of  $I_0$  is 22.4 drops/cm and the italicized assignments are made.

Track No.	$P(\text{Mev}/c)$	$I(\text{drops}/\text{cm})$	$I_{0e}$	$I_{0\pi}$	$I_{0K}$	$I_{0p}$	Particle
1	94.6	31.5	21.7	12.4	...	...	$e^+$
2	2341	25.3	15.6	22.0	25.3	24.6	$\pi^-$
3	3040	23.5	14.5	19.8	22.7	23.5	$K^+$ (or $p$ )
4	2888	27.6	17.0	23.3	26.9	27.3	$\pi^-$
5	3185	23.3	14.4	19.6	22.5	23.3	$K^+$ (or $p$ )
6	2644	35.3	21.8	30.3	34.8	35.0	$e^+$
7	7358	28.6	17.7	22.0	25.2	27.0	$\pi^+$

determination of  $I_0$  from adjacent electron showers was often useful, as well as intercomparison of tracks in a given penetrating shower. We have taken 5% as the standard error in ionization measurements of all full-length tracks.

### Identification of the Particles

The procedure on identification of particles in a penetrating shower is illustrated in Table I (Event 73309). The momentum and ionization for each particle are given in the table. With the aid of the experimentally determined curve of ionization versus  $\beta\gamma$  [ $\beta=v/c$  and  $\gamma=(1-\beta^2)^{-1/2}$ ], the hypothetical value of  $I_0$  is determined for various possible particles. For example,  $I_{0e}$  is the value of  $I_0$  that would have had to exist in the chamber if the particle had been an electron,  $I_{0\pi}$  for a  $\pi$  meson, etc. It is seen that the most consistent values of  $I_0$  obtained are *italicized*, giving an average  $I_0$  of 22.4 drops/cm. That this is the correct value is substantiated by measurements on the electron shower event 73303, which gave a value of 22.8 drops/cm. The separation between electron and pion is good, and likewise between pion and proton, but the  $K$  meson and proton cannot be distinguished in individual cases. For purposes of analysis, however, the particle which yields the closest value of  $I_0$  is chosen, either proton or  $K$  meson.

The degree of uncertainty in the identification of the particles depends not only on the ionization error but also on the error made in the determination of the momentum. Figure 2 shows the ionization versus momentum curves for various particles, together with the momentum error at several values of the momentum. The ionization error is shown as 5% and is practically independent of the momentum. Separation of pions from protons at 10 Bev/ $c$  is evident.

The degree of certainty of separation of particles at three different momenta is shown in Fig. 3. These curves show the value of the ratio  $I/I_0$  for a given particle at a given momentum, calculated for the predicted value at that momentum, and for values differing from the predicted value by 0.5, 1, 1.5, etc., standard deviations. Thus, for example, at 5 Bev the proton and pion curves intersect at about  $2\sigma$ , giving an excellent separation of these two types of particles.

At 20 Bev they overlap at about  $1\sigma$ , because of increased errors in the momentum determination. Protons and  $K$  mesons are not clearly distinguished in individual cases at any of these momenta. Electrons can be distinguished from pions up to about 20 Bev.

In the showers observed, only 13 particles had momenta greater than 20 Bev/ $c$ , and even for some of these, which were of momentum greater than 30 Bev/ $c$ , it was possible to make a tentative assignment of identity on the basis of ionization measurements. The general procedure was to identify particles according to their most probable identity, since we did not feel it was necessary to verify the fact that  $K$  particles and negative protons exist.

### Angle Determinations

The angle of emission of each secondary particle with respect to the direction of the primary particle producing the nuclear interactions is a basic datum for all calculations on a penetrating shower. The experimental arrangement used did not give the direction of the primary. We decided that the best approximation to the direction of the primary would be the direction of the total momentum of all the secondaries. No systematic error is to be expected in this approximation, but fluctuations in a single event can be appreciable, especially if a neutral particle carries off a large amount of momentum. For this reason, no results referring to an individual event will be given, and the final results

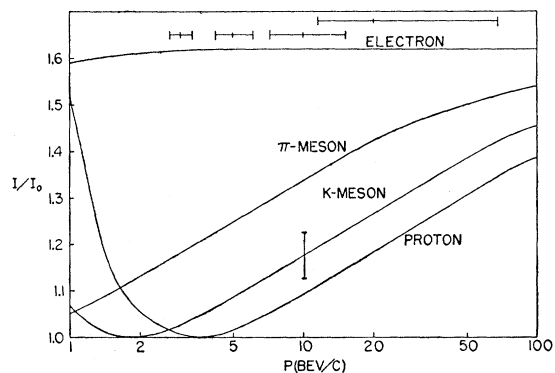


FIG. 2. Ionization vs momentum for relativistic particles.

will refer to average values over groups of showers. There is considerable theoretical justification for this procedure, since the impact parameter in a given collision cannot be known in any case, and the theories also predict average behavior over various impact parameters.

The space angles of the particles were measured on a stereoscopic projector and space table. The system of coordinates was defined such that the  $xy$  plane corresponded to the back plate of the chamber, and the  $z$  axis was normal to the back plate at the center. With respect to this system, the angle  $\eta'$  that the projection of the track formed with the  $y$  axis, and the angle  $\varphi$  that the track formed with the  $z$  axis, were measured. All angles were measured twice and the estimated errors were

$$\pm 0.5^\circ \text{ for } \eta' \text{ and } \pm 1.5^\circ \text{ for } \varphi.$$

The angle  $\eta'$  was corrected to take into account the deflection in the magnetic field before the particle entered the chamber, giving a corrected value  $\eta$  for this angle.

The values of  $\eta$  and  $\varphi$ , together with the value of the momentum  $p$  for each track, were then combined to give the direction of the total momentum and the angle  $\theta$  between each track and the direction of the total momentum. This was the first step in the program developed for the analysis of the events.

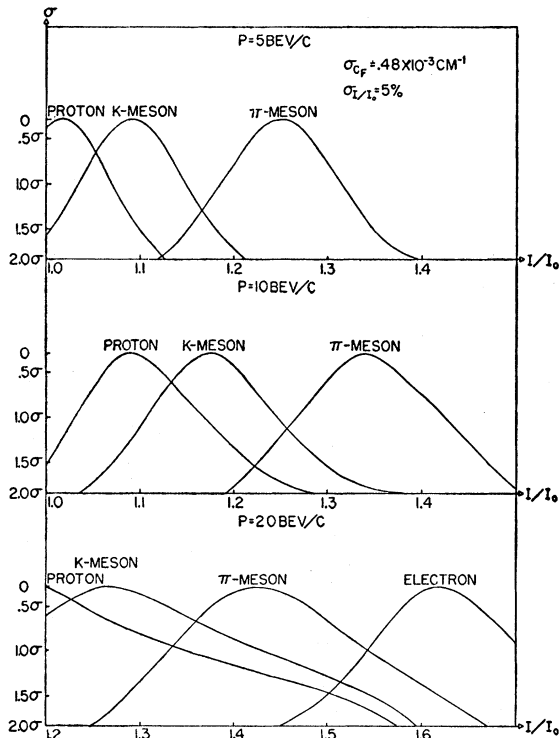


FIG. 3. Degree of identification of particles by ionization for a given momentum, taking into account the errors in ionization and momentum.  $\sigma_{CF}$  is the standard error in track curvature.

#### DETERMINATION OF THE VELOCITY OF THE CENTER OF MASS

The second step in the program was to calculate the velocity of the center of mass  $\beta_c$  of the particle causing the event. Various procedures<sup>5,8,9</sup> have been developed to determine the velocity of the center of mass in such collisions, using angle measurements and Lorentz transformations. A disadvantage of the present experiment is the possibility that one or more particles can escape being seen in the cloud chamber, if they are emitted at large angles. In a nuclear emulsion, all charged particles are seen. An important advantage of the present experiment is that both the momentum and energy of the particles can be determined, since the identities are known.

For each particle the value of  $p_i$ , and its component  $p_{ix} = p_i \cos\theta_i$ , and  $E_i = (p_i^2 + m_i^2 c^4)^{1/2}$  are known in the laboratory system. According to the Lorentz transformation,  $p_{ix}'$  in the center-of-mass system is given by  $p_{ix}' = \gamma_c (p_{ix} - \beta_c E_i/c)$ .

In the center-of-mass (c.m.) system the sum of the longitudinal components of the momentum is zero. Hence

$$\sum_{i=1}^n p_{ix}' = 0 = \sum_{i=1}^n \gamma_c (p_{ix} - \beta_c E_i/c).$$

Thus

$$\beta_c = \frac{\sum_{i=1}^n c p_{ix} / \sum_{i=1}^n E_i. \quad (1)$$

This equation is strictly true for collisions of any kind, and is not restricted to nucleon-nucleon collisions. The summation must be made over all particles, charged and neutral. It is reasonable to assume from symmetry arguments, however, that on the average over a number of showers, Eq. (1) should hold independently for charged particles and neutral particles. The procedure was therefore to calculate  $\beta_c$  (and hence  $\gamma_c$ ) using the data available on charged secondaries.

A possible source of systematic error in the determination of  $\gamma_c$  by this method is due to the geometry of the chamber and the target material, which was above the chamber. If a particle were emitted at such an angle that it would not traverse the chamber, it would not be seen, and hence would not be included in the calculation. The systematic omission of such particles from the calculation will have a systematic effect on the values of  $\gamma_c$  obtained. The importance of this effect depends on the height above the chamber where the event occurs, and the energy of the event. Table II gives the distribution of events in the carbon and the maximum detectable angles in breadth and depth for the given height, assuming that the event occurred in the center line of the apparatus. It is seen

<sup>8</sup> C. Castagnoli, G. Cortini, C. Franzenetti, A. Manfredini, and D. Moreno, Nuovo cimento **10**, 1539 (1953).

<sup>9</sup> F. H. Tchang, C. C. Dilworth, S. I. Goldsack, T. F. Hoang, and L. Scarsi, Nuovo cimento **10**, 1261 (1953); **11**, 424 (1954).

TABLE II. Distribution of events in the producing layer of carbon.

$h$ (cm)	Max. angle in depth	Max. angle in breadth	Number of events
5	30°	60°	12 under 5 cm
10	22°	50°	11 between 5-10 cm
15	19°	43°	3 between 10-15 cm
20	15°	37°	6 between 15-20 cm
25	13°	32°	3 between 20-25 cm
30	11°	29°	2 between 25-30 cm
35	10°	26°	2 between 30-35 cm
40	9°	23°	2 between 35-40 cm

that over half of the events occur in the 15 cm of carbon nearest the chamber, which is understandable because of the counter bias.

The effect of the energy on the opening angle of the shower is shown in Fig. 4, which was calculated assuming an isotropic angular distribution of the secondaries in the c.m. system. Comparison of Fig. 4 with the angles of Table II indicates that at low energies at least, there is quite an appreciable probability of missing particles. We therefore also calculated values of  $\gamma_c$  for the following hypotheses:

$\gamma_I$ : obtained from the balance of momentum of the visible particles.

$\gamma_{I-1}$ : obtained as above, but adding one particle of energy 1 Bev at 15° in the laboratory system.

$\gamma_{I-2}$ : obtained as above, but adding one 1-Bev particle at 15° and one 1-Bev particle at 20° in the laboratory system.

The effect of missing particles is thus estimated.

The values of  $\gamma_c$  were also calculated by methods previously used where symmetry in the c.m. system is assumed.

Castagnoli et al.,<sup>8</sup> used

$$\log \gamma_c = -\frac{1}{n} \sum_{i=1}^n \log |\tan \theta_i|, \quad (2)$$

and Hoang et al.,<sup>9</sup> used

$$1/\gamma_c^2 = \tan \theta_f \tan \theta_{1-f}, \quad (3)$$

where  $\theta_f$  is the angle that includes a fraction  $f$  of the particles in the laboratory system, and  $\theta_{1-f}$  includes the remainder of the particles.

These results are all collected in Table III. Examination of this table reveals the following general observations.

1. The geometric bias is much more important for low energies than high energies.

2. In most cases the values of  $\gamma_{II}$  and  $\gamma_{III}$  are larger than  $\gamma_I$ . A similar observation was made by Gramonizky et al.,<sup>10</sup> indicating that these purely geometrical procedures give systematically high values of  $\gamma$ .

<sup>10</sup> I. M. Gramonizky, G. B. Zdanov, E. A. Zamcalova, M. I. Tretjakova, M. N. Scerbakova, Suppl. Nuovo cimento 8, 714, 727 (1958).

3. The value of  $\gamma_I$  is expected to be systematically *smaller* than the true value for the highest energy events. The reason for this, and also the reason for the fact that the visible secondary energy in the highest energy events is much less than the assigned primary energy, is that the maximum detectable momentum in the cloud chamber is about 30 Bev/ $c$ . Thus in a high-energy interaction, where one of the particles retains much of the initial energy, that particle will not, on the average, yield a measured momentum of much more than 30 Bev/ $c$ . In the calculation of  $\beta_c$  from Eq. (1), neglect of large, essentially equal terms in numerator and denominator can only reduce the apparent value of  $\beta_c$  and hence  $\gamma_c$ . If the bulk of the energy is carried

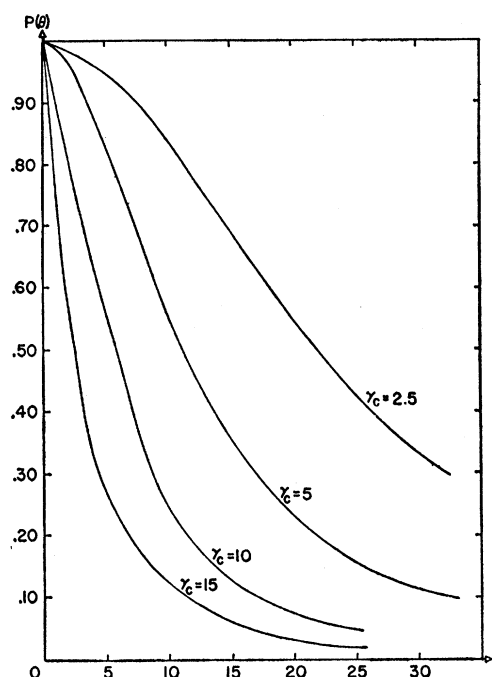


FIG. 4. Effect of energy on the opening angle of the shower, assuming an isotropic angular distribution of the secondaries in the c.m. system.

off by a neutral particle, the same effects will be produced.

The value of  $\gamma_c$  taken for the present analysis was  $\gamma_I$  except for those cases where the origin of the shower was higher than 20 cm above the top of the chamber, in which case  $\gamma_{I-1}$  or  $\gamma_{I-2}$  was taken. We estimate the average error in  $\gamma_c$  to be about  $\pm 30\%$  under this procedure.

Once the value of  $\gamma_c$  was determined the energies, momenta, and angles in the c.m. system were determined for the secondary particles by means of the Lorentz transformations. The calculations were performed on an IBM 701.

TABLE III. Information on individual events. The value of  $\gamma$  adopted for the analysis is italicized.

	Height above top of chamber (cm)	Total energy of visible particles (Bev)	$n_s$	$\gamma_I$	$\gamma_{I-1}$	$\gamma_{I-2}$	$\gamma_{II}$	$\gamma_{III}$	$K_L$	$K_c$
75174	34	22.7 <sup>+</sup> <sub>-</sub> 18.0 3.8	5	7.6	6.9	<i>5.9</i>	12.0	10.3	0.457	0.542
75300	7	18.9 <sup>+</sup> <sub>-</sub> 3.5 2.6	6	<i>8.4</i>	7.3	6.0	6.5	7.5	0.216	0.244
75468	3	8.9 <sup>+</sup> <sub>-</sub> 1.7 1.2	3	<i>4.8</i>	4.5	4.0	6.1	10.8	0.310	0.383
75622	5	89.5 <sup>+</sup> <sub>-</sub> 51.1 32.1	5	45.8	<i>36.9</i>	27.2	32.5	43.9	0.064	0.066
75733	30	26.3 <sup>+</sup> <sub>-</sub> 12.0 6.0	4	13.0	10.1	<i>7.8</i>	9.7	10.9	0.397	0.450
75758	3	23.9 <sup>+</sup> <sub>-</sub> 6.6 3.9	5	<i>7.8</i>	7.1	6.1	6.4	10.5	0.349	0.396
76296	20	23.1 <sup>+</sup> <sub>-</sub> 10.7 4.9	5	<i>6.3</i>	5.9	5.3	9.3	6.2	0.310	0.354
76375	16	15.6 <sup>+</sup> <sub>-</sub> 3.8 2.8	5	<i>9.7</i>	7.8	6.1	7.4	10.7	0.207	0.227
76485	25	134.6 <sup>+</sup> <sub>-</sub> 104.8 45.8	6	36.2	32.7	<i>27.3</i>	73.0	35.0	0.086	0.089
77027	1	82.8 <sup>+</sup> <sub>-</sub> 62.5 27.8	5	<i>34.7</i>	33.9	21.3	78.5	70.7	0.054	0.056
77147a	3	18.3 <sup>+</sup> <sub>-</sub> 3.9 3.0	4	<i>12.7</i>	9.3	6.9	8.9	15.0	0.144	0.156
77147b	In chamber	12.4 <sup>+</sup> <sub>-</sub> 4.6 2.5	4	<i>3.0</i>	...	...	11.7	8.1	0.828	1.018
77548	22	14.4 <sup>+</sup> <sub>-</sub> 4.0 2.4	3	4.5	4.4	<i>4.0</i>	15.6	20.0	0.573	0.740
77817	20	59.2 <sup>+</sup> <sub>-</sub> 33.2 13.8	10	<i>9.1</i>	9.1	8.8	14.4	10.9	0.483	0.539
77835	20	21.7 <sup>+</sup> <sub>-</sub> 4.6 3.2	6	7.0	6.4	5.6	8.2	7.7	0.335	0.381
77981	6	10.9 <sup>+</sup> <sub>-</sub> 1.8 1.3	3	13.8	8.5	<i>6.0</i>	12.2	15.0	0.244	0.279
78273	7	24.0 <sup>+</sup> <sub>-</sub> 32.3 7.8	3	14.2	<i>10.5</i>	7.8	12.5	10.8	0.034	0.040
69830	6	5.0 <sup>+</sup> <sub>-</sub> 0.4 0.3	3	8.4	5.9	2.3	9.4	15.0	0.827	1.323
69846	35	18.6 <sup>+</sup> <sub>-</sub> 5.2 3.0	4	4.7	4.6	<i>4.4</i>	10.7	16.8	0.327	0.488
69857	2	73.2 <sup>+</sup> <sub>-</sub> 47.4 12.0	8	<i>15.6</i>	13.4	11.0	22.2	10.5	0.161	0.208
69979	7	55.7 <sup>+</sup> <sub>-</sub> 37.1 14.9	6	<i>9.4</i>	8.5	7.4	6.9	15.2	0.361	0.404

## TRANSVERSE MOMENTUM DISTRIBUTION

### Experimental Results

The theories of high-energy nuclear collisions each predict the distribution of  $p_T$ , the transverse momentum of the secondary particles. The  $p_T$  distribution obtained in this experiment is shown in Fig. 5. The most probable value of  $p_T$  lies between  $m_\pi c$  and  $2m_\pi c$ , and the average value for all secondaries is

$$\bar{p}_T = (308 \pm 23) \text{ Mev}/c \quad \text{or} \quad (2.2 \pm 0.2)m_\pi c.$$

If the secondary particles are divided into light and heavy particles before the average is taken, the results are:

$$\bar{p}_T = (310 \pm 44) \text{ Mev}/c \quad \text{for the heavy particles} \\ \text{(protons and } K \text{ mesons),}$$

$$\bar{p}_T = (307 \pm 26) \text{ Mev}/c \quad \text{for the pions.}$$

Grouping of the particles from high- and low-energy showers shows that  $\bar{p}_T$  is independent of primary and secondary energies. These results are similar to those obtained previously in photographic emulsions.<sup>11</sup>

### Comparison with Theory

The low values found for  $\bar{p}_T$  and the independence of  $\bar{p}_T$  of the energy of the primary are inconsistent with the Fermi theory,<sup>12</sup> which predicts a very high value for  $p_T$  (several Bev/ $c$ ) for high-energy interactions.

In the original Landau theory,<sup>13</sup> the initial state of the high-energy collision is the same as the Fermi model. Following this is a second state, corresponding to a one-dimensional expansion of the system, when the

<sup>11</sup> *International Congress in Cosmic Rays* [Suppl. Nuovo cimento, 8, 710 ff (1958)].

<sup>12</sup> E. Fermi, Phys. Rev. 81, 683 (1951).

<sup>13</sup> S. Z. Belenky and L. D. Landau, Suppl. Nuovo cimento 1, 15 (1956).

TABLE III.—Continued.

	Height above top of chamber (cm)	Total energy of visible particles (Bev)	$n_s$	$\gamma_I$	$\gamma_{I-1}$	$\gamma_{I-2}$	$\gamma_{II}$	$\gamma_{III}$	$K_L$	$K_e$
71885	17	15.7 <sup>+</sup> <sub>3.1</sub>	3	9.9	7.9	6.2	13.6	12.0	0.105	0.120
71991	4	23.8 <sup>+</sup> <sub>6.8</sub>	3	9.7	8.3	6.8	6.5	10.6	0.173	0.190
72695	14	7.7 <sup>+</sup> <sub>0.6</sub>	5	4.6	4.4	2.6	3.7	7.5	0.325	0.389
73303	18	27.3 <sup>+</sup> <sub>6.2</sub>	4	6.8	6.4	5.8	7.2	13.9	0.274	0.317
73309	7	24.2 <sup>+</sup> <sub>3.3</sub>	6	5.7	5.5	5.0	8.1	14.0	0.597	0.710
73615	8	13.0 <sup>+</sup> <sub>1.6</sub>	4	4.9	4.7	4.3	5.6	12.7	0.456	0.556
73672	8	72.3 <sup>+</sup> <sub>18.7</sub>	6	23.1	17.2	12.0	17.0	14.4	0.109	0.114
73682a	40	13.5 <sup>+</sup> <sub>1.5</sub>	5	16.7	9.6	6.6	24.0	32.0	0.560	0.650
73682b	13	21.8 <sup>+</sup> <sub>4.2</sub>	4	7.3	6.7	5.8	15.6	14.6	0.204	0.232
73857	8	18.8 <sup>+</sup> <sub>5.0</sub>	3	13.8	9.7	7.1	22.4	19.2	0.077	0.088
74004	10	5.4 <sup>+</sup> <sub>0.4</sub>	3	1.9	1.8	1.7	6.7	13.5	1.307	1.570
74064	40	38.4 <sup>+</sup> <sub>12.1</sub>	4	10.7	9.4	7.9	8.4	14.9	0.394	0.447
74080	4	36.9 <sup>+</sup> <sub>9.7</sub>	6	7.2	6.8	6.2	8.8	10.9	0.611	0.684
74337	2	48.2 <sup>+</sup> <sub>15.1</sub>	6	4.6	4.6	4.4	4.4	6.4	0.618	0.894
74453	3	21.6 <sup>+</sup> <sub>4.0</sub>	5	6.9	5.8	5.2	7.8	18.0	0.347	0.401
74571	31	22.7 <sup>+</sup> <sub>5.2</sub>	3	12.4	9.6	7.1	23.9	24.5	0.244	0.278
74609	23	41.5 <sup>+</sup> <sub>20.7</sub>	3	7.4	7.0	6.4	17.7	14.7	0.661	0.750
74796	7	41.0 <sup>+</sup> <sub>10.2</sub>	5	12.3	10.5	8.6	11.5	7.7	0.076	0.082
74950	21	14.1 <sup>+</sup> <sub>2.8</sub>	3	8.1	6.9	5.6	12.0	15.2	0.269	0.322
75139	3	16.3 <sup>+</sup> <sub>2.0</sub>	3	3.5	3.4	3.0	4.6	5.8	0.711	0.868

temperature drops from the initial  $T_0$  to a lower  $T_1$ . The system then expands conically and the temperature drops to  $T_f$ , the breakup temperature, which is of the order of  $m_\pi c^2/k$ . The transverse momentum of the

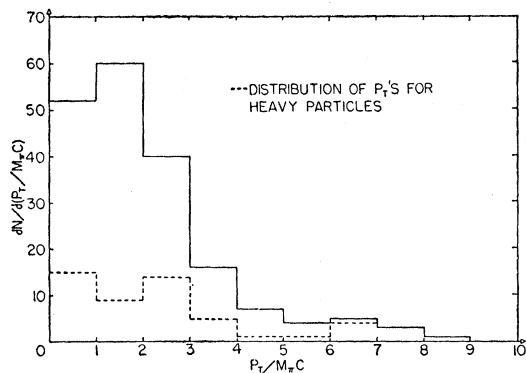


FIG. 5. Distribution of transverse momentum of the secondary particles. The distribution for the heavy particles alone is given by the dotted line.

particles is determined in the original Landau theory by the value of  $T_1$ , and gives  $\bar{p}_T$  of the order of  $M c$ , where  $M$  is the nucleon mass, well above the experimental results.

A modification of the Landau three-state treatment has been suggested by Melečín and Rozental.<sup>14</sup> They state that for energies below  $10^{13}$  ev a good treatment of the high-energy collision can be made without introducing the three-dimensional stage, which is important only for energies  $> 10^{14}$  ev. The curves given by Melečín and Rozental for the resultant  $\bar{p}_T$  distribution are drawn on Fig. 6, normalized to fit the present data on the  $\bar{p}_T$  distribution for the pions. It is seen that the best fit corresponds to the distribution curve for  $T_f = m_\pi c^2/k$ . The same result was found by these authors for the distribution of transverse momentum given by Debenedetti et al,<sup>15</sup> and Zdanov

<sup>14</sup> G. A. Melečín and I. L. Rozental, Suppl. Nuovo cimento **8**, 770 (1958).

<sup>15</sup> A. D. Debenedetti, C. M. Garelli, L. Tallone, and M. Vigone, Nuovo cimento **4**, 1142 (1956).

et al.<sup>10</sup> Thus the one-dimensional approximation method appears to work well at these energies.

In the Heisenberg theory<sup>16</sup> the predicted value of  $\bar{p}_T$  is  $m_\pi c$ , which is smaller than the experimental value.

**ENERGIES OF THE SECONDARIES IN THE C.M. SYSTEM**

The total energies of the particles in the c.m. system were obtained from the relation  $E_i' = \gamma_c(E_i - \beta_c p_{i,c} \cos \theta_i)$ , and are plotted in Fig. 7. The heavy particles and light particles have quite different energy spectra. Since most theories predict that the average energy in the c.m. system will increase with primary energy, the distribution of the pion energies has been plotted for two different energy groups in Fig. 8. The curves drawn are calculated according to Heisenberg's theory. The average energies for pions in the present experiment are compared with the theoretical predictions in Table IV. No significance is attached to the decrease in the

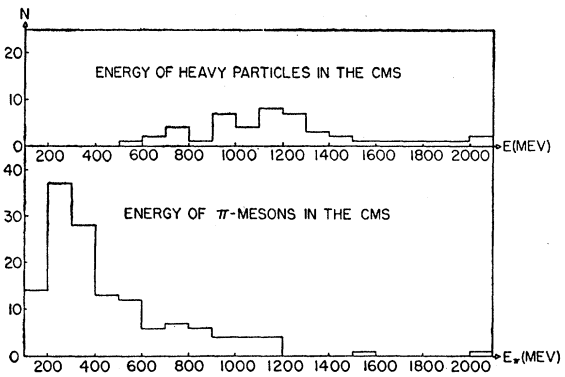


FIG. 7. Total energies of particles in the c.m. system.

pion energies of this order of magnitude. The Heisenberg theory seems to give a better prediction of the energy spectrum, which goes as  $1/E^2$  in the Heisenberg theory, and  $1/E$  in the Landau theory.

The average energy of the heavy particles in this experiment was  $(1260 \pm 200)$  Mev for 28 events with  $\gamma_c < 10$ . Heisenberg's theory gives 1030 Mev for the average energy of *K* mesons produced in collisions of this energy. However, since the *K* mesons were not separated from the protons, no conclusions are made except that the energies of heavy particles are of the right order of magnitude to agree with Heisenberg's theory.

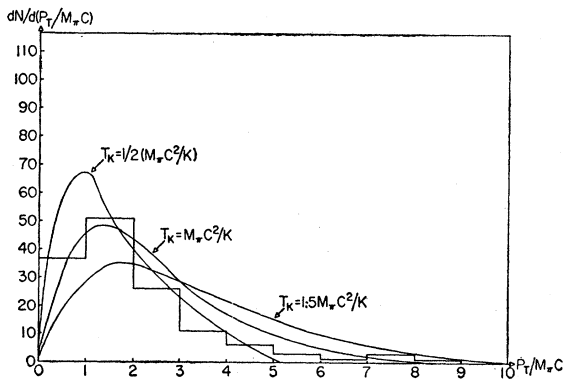


FIG. 6. Distribution of transverse momentum of the pions, compared to curves given by Melečín and Rozental.

experimental value between  $\gamma_c = 7$  and  $\gamma_c = 25$  because of the experimental errors.

The original Fermi predictions are not compatible with the present experimental results, or the results from emulsions, although the predicted value for  $E_\pi$  can be brought down if the radius of the Fermi volume of interaction is increased and the production of *K* mesons is taken into account as has been shown by Kretzschmar.<sup>17</sup>

Landau's value for  $\bar{E}_\pi$  is a function of the break-down temperature of the system. If the value of  $T_f$  is taken from the distribution of transverse momenta (according to the modified model of Melečín and Rozental) as  $T_f = m_\pi c^2/k$ , the value of  $\bar{E}_\pi$  for pions produced by primaries of energies in the interval  $10^{10}$  to  $10^{12}$  ev is  $\bar{E}_\pi = 460$  Mev, consistent with the experimental value. Numerous emulsion studies have also given average

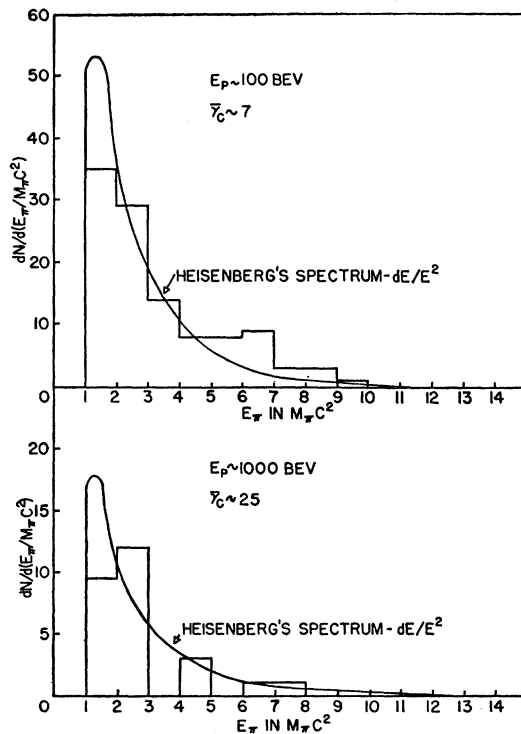


FIG. 8. Energy spectrum of pions in the c.m. system compared to Heisenberg's theory.

<sup>16</sup> W. Heisenberg, Nature 65, (1949); Z. Physik 126, 569 (1949); Z. Physik 133, 65 (1952).

<sup>17</sup> M. Kretzschmar, Z. Physik 150, 247 (1958).



TABLE IV. Comparison of the experimental values of average pion energy with the theoretical predictions.

	$E_p = 100$ Bev	$E_p = 1000$ Bev
Present experiment	$470 \pm 50$ (Mev)	$370 \pm 80$
Heisenberg <sup>a</sup>	400	550
Fermi	2550	4850
Landau ( $T_f = m_\pi c^2/k$ )	460	460

<sup>a</sup> See reference 15.

#### ANGULAR DISTRIBUTION OF THE SECONDARIES

The emission angle of the secondaries in the center-of-mass system was calculated according to the transformation equation

$$\tan\theta_i' = \frac{\tan\theta_i}{\gamma_c [1 - (\beta_c/\beta_i) \sec\theta_i]}$$

Figure 9 shows the angular distribution of the  $\pi$  mesons in the center-of-mass system. The only events considered for the plot of angular distribution were those with four or more secondaries. There were 29 such events. The full curve represents the distribution of the  $\pi$  mesons produced by primaries with  $\gamma_c < 15$ . The dotted curve corresponds to five events with  $\gamma_c > 15$ . Both distributions are anisotropic and seem to increase in the degree of anisotropy with the energy of the primary. However, this increase is not certain because of the small number of tracks involved in the second distribution.

The angular distributions predicted by the theories of Landau and Heisenberg are anisotropic, the degree of anisotropy increasing with the primary energy. In Heisenberg's theory the anisotropy in the angular distribution appears at energies higher than  $10^{12}$  ev, while at lower energies the angular distribution can be approximated by an isotropic distribution.

The two angular distributions do seem to show a certain anisotropy which, if it is a real effect, does not

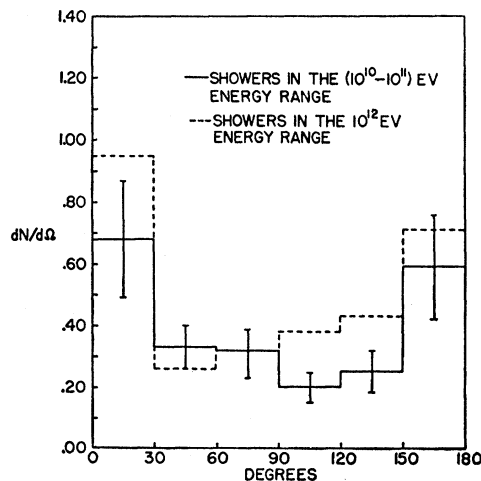


FIG. 9. Angular distribution of pions in the c.m. system.

agree with the isotropic distributions predicted by Heisenberg for the range of primary energies observed, but does agree with the Landau predictions. Results on the degree of anisotropy of the angular distribution with much better statistics than the present work, but not yet conclusive enough to be able to make a sharp differentiation between Heisenberg and Landau's predictions, have been reported by Lindern,<sup>18</sup> Ciok et al.,<sup>19</sup> and Bozoki et al.<sup>20</sup>

The angular distribution of the heavy particles in the center-of-mass system can be seen in Fig. 10. The degree of anisotropy of this distribution is larger than the anisotropy shown by the  $\pi$ -meson angular distribution of Fig. 9 by a factor of 3 or 4. A tentative identification of some  $K$  mesons among the heavy particles was attempted, giving the dotted line in Fig. 10 corresponding to the angular distribution of possible  $K$  mesons. The spectrum of energy of the heavy particles (Fig. 7) shows that the  $K$  mesons have a higher energy than the  $\pi$  mesons in the c.m. system. The larger

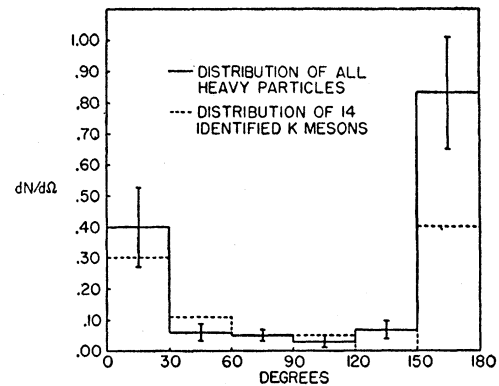


FIG. 10. Angular distribution of heavy particles in the c.m. system.

anisotropy observed in their angular distribution is associated with their higher energy in the c.m. system, as has been stated by Heisenberg.

#### ENERGIES OF THE PRIMARIES AND THE INELASTICITY OF THE COLLISIONS

The inelasticity  $K$  of the collision is one of the most significant parameters in the study of high-energy interactions.  $K$  is defined as the ratio of the total energy of all particles created in the collision to the total available kinetic energy of the colliding particles. It is thus necessary to determine the energy of the primary particle, which is obtained from a knowledge of  $\gamma_c$  and an assumption on the nature of the particles involved

<sup>18</sup> L. V. Lindern, Nuovo cimento 5, 491 (1957).

<sup>19</sup> P. Ciok, T. Coghén, J. Gierula, R. Holynski, A. Jurak, M. Miesowicz, T. Saniewska, and O. Stanis, Nuovo cimento 10, 741 (1958).

<sup>20</sup> G. Bozoki, E. Fenyves, E. Gombosi, Nuclear Phys. 8, 199 (1958).

in the collision. For a nucleon-nucleon collision, in the c.m. system,

$$K_c = \sum E_i / 2Mc^2(\gamma_c - 1),$$

and for a pion-nucleon collision,

$$K_c = \sum E_i / (2Mc^2\gamma_c - Mc^2 - m_\pi c^2).$$

Another determination of  $K$  can be made by measurement of the energies in the laboratory system. For either nucleon-nucleon collisions, or pion-nucleon collisions at these energies

$$K_L = \sum E_i / Mc^2(2\gamma_c^2 - 1).$$

In all these expressions the numerators indicate summations over the created particles. It is seen that for large values of  $\gamma_c$ , including most of those observed in this experiment, the assumption of either a nucleon or a pion as the incident particle will not appreciably affect the values of  $K$  obtained.

We have assumed nucleon-nucleon collisions and have taken into account the created particles in the following way.

1. The total energy in the pions was taken as 1.5 times the total energy in the observed charged pions, to account for the neutral pions.

2. As is discussed later, strange particles are produced in relatively small numbers. We therefore assumed that: (a) all negative heavy particles are  $K$  mesons (there were 13 such particles); (b) positive heavy particles in the forward cone with energies in the laboratory system more than 3 times the highest energy pion produced in the collision were considered as primary protons and not included among the secondaries (there were 10 such particles); (c) where two positive heavy particles were in the backward cone, one was taken as the target nucleon, and the other as a  $K^+$  meson; and (d) if only one positive heavy particle was in the backward cone, it was assumed to be the target nucleon. Alternate calculations were also made assuming it was a  $K^+$  meson, and no significant difference was found in the value of  $K$ .

The energy in the  $K$  mesons was then taken as 2 times the energy in the charged  $K$  particles to take into account the two neutral states of the  $K$  meson.

These results are shown in Table III and in Fig. 11. The theoretical curve predicted by Heisenberg is shown in Fig. 11. The values of  $K_c$  and  $K_L$  differ by a factor which decreases as  $\gamma_c$  increases. The decrease of  $K$  with energy is evident, and at the higher values of  $\gamma_c$ , the experimental results of  $\bar{K}_c$  agree well with the Heisenberg theory.

If more than one target nucleon were involved in the collision, the inelasticities would be correspondingly reduced. The low values obtained argue against the involvement of many nucleons in the collision.

The energy distribution of the events should be compared with a predicted distribution based on the detection characteristics of the cloud chamber ap-

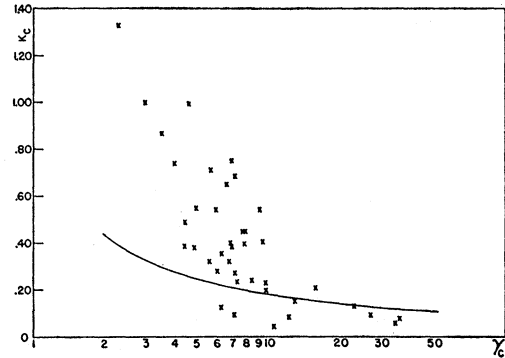


FIG. 11. Inelasticity vs  $\gamma_c$ .

paratus, and the energy spectrum of the primary particles. Unfortunately, both of these are quite uncertain. The cloud-chamber triggering device becomes more sensitive with increasing primary energy, which produces greater concentration of the secondaries on the Geiger counters, and increasing multiplicities of the secondaries, but this effect cannot be calculated accurately. The spectrum of nuclear-active particles is known only by extrapolation from experiments by Mylroi and Wilson<sup>21</sup> and by Bridge and Rediker<sup>22</sup> in the energy range up to 10 or 20 Bev. With all these uncertainties we have attempted to calculate the predicted number of events in various energy ranges, and compare this with the actual number observed, assuming that the struck particle was in each case a nucleon. With the possible exception of the energy range above 1000 Bev, the predicted and observed rates agreed to a factor of two. The likely increase in the number of primary pions at very high energies even makes the 1000-Bev figure possible.

#### MULTIPLICITY

The number of charged particles observed as a function  $\gamma_c$  is shown in Table V. The most striking fact about these observations is the small number of particles observed compared with the multiplicities of jets in emulsions at comparable energies. Thus the recent work of Ivanovskaya and Chernavsky<sup>23</sup> and of Gozani and Sitte,<sup>24</sup> which emphasize the nucleon-nucleus character

TABLE V. Multiplicity of particles as a function of energy of the primary.

$\bar{\gamma}_c$	2.7	7	23
$N_i$ (experimental)	$4.0 \pm 1.1$	$7.4 \pm 0.5$	$9.9 \pm 1.4$
$N_i$ (Landau-Belenky $C=1.5$ )	3.2	6.5	11.6
$N_\pi$ (total) exper.	$2.3 \pm 0.8$	$5.0 \pm 0.4$	$7.8 \pm 1.2$
$N_\pi$ (total) Heisenberg	$3.6 \pm 0.7$	$4.2 \pm 0.8$	$5.2 \pm 0.8$

<sup>21</sup> M. G. Mylroi and J. G. Wilson, Proc. Phys. Soc. (London) **A64**, 404 (1951).

<sup>22</sup> H. S. Bridge and R. H. Rediker, Phys. Rev. **88**, 206 (1952).

<sup>23</sup> I. A. Ivanovskaya and D. S. Chernavsky, Nuclear Phys. **4**, 29 (1957).

<sup>24</sup> T. Gozani and K. Sitte, Nuovo cimento **11**, 26 (1959).

of most collisions in emulsions, is confirmed. The largest number of penetrating particles observed in an event in this experiment was 10, whereas multiplicities in photographic emulsion at 1000 Bev are usually at least 20.

At low energies the results are not certain because of the experimental bias. On the one hand, no showers with fewer than three charged penetrating particles are included in this analysis, although many were observed. On the other hand, particles may readily miss the cloud chamber if they are emitted at large angles, which is more likely at low energies. Thus the two effects tend to compensate, but the result at low  $\gamma_c$  remains uncertain. In addition to this, only three events are included in the low  $\gamma_c$  group.

The results can be compared to the predictions of the Landau and Heisenberg theories. We take

$$N_t = 1.5n_{\pi^+} + 2n_{h.p.},$$

where  $n_{h.p.}$  is the number of charged heavy particles observed.

In the Landau theory  $N_t = A^{0.19}N_0$ , where  $A$  is the mass number of the element in which the collision occurred and  $N_0$  is the number of secondaries emitted in a nucleon-nucleon collision. The dependence of the multiplicity on the nuclear mass has been calculated by Belenky et al.<sup>26</sup> For carbon the result is  $N_t = 1.6C \times (E_p/2Mc^2)^{1/2}$  where  $C$  is an adjustable constant of the order of 2. The experimental results and the results of the Landau-Belenky calculation with  $C = 1.5$  are shown in Table V.

The multiplicities in the Heisenberg theory were obtained from the expression

$$n_i = \frac{E(g_i/m_i c^2)(4/\pi)[1 + 2\alpha_i^2 - 2\alpha_i(1 + \alpha_i^2)^{1/2}]}{\sum g_i(-1 + (1 + \alpha_i^2)^{1/2} \ln\{[1 + (1 + \alpha_i^2)^{1/2}]/\alpha_i\})},$$

where  $n_i$  is the number of particles of type  $i$ ,

$$\sum g_i = 1, \quad (g_\pi = \frac{1}{3}, g_K = \frac{2}{3}), \quad \alpha_i = (m_i c^2 / m_\pi c^2 \gamma_c) K,$$

$E = 2M_c^2(\gamma_c - 1)K$ . The values used for  $K$  were the theoretical values of the inelasticity predicted by the Heisenberg theory for each energy range. Thus there are no adjustable constants in the Heisenberg predictions of multiplicity. It is seen that both the Heisenberg predictions and the Landau-Belenky predictions are in agreement with the experimental results.

We have also compared our results with the calculations of Ivanovskaya and Chernavsky<sup>23</sup> to determine the number of nucleons usually involved in a collision in carbon. Figure 12 shows the curves calculated by Ivanovskaya and Chernavsky using the statistical theory predictions of multiplicities of production in nucleon-nucleus collisions. These curves give the number of nucleons involved in the collision for a given

value of  $\gamma_c$  when  $N_s$  charged particles are produced in the collision. In this figure the positions of the 41 events included in this work are shown. Most of them fall near the curve  $N=2$ , which corresponds to one nucleon of the target plus the incident nucleon.

An experimental argument against the participation of many of the target nucleons in the collision comes from the small number of positive heavy particles observed to emerge from the interactions. In the 41 interactions, only 32 positive heavy particles were observed, and as will be seen in the next section, it is reasonable to assume that some of these are positive  $K$  mesons. Thus the total number of protons observed is of the order of one-half the number of interactions, and one can conclude that not many multiple-nucleon processes could have occurred.

### STRANGE PARTICLES

The forty-one events analyzed included 144  $\pi^\pm$  mesons and 48 heavy particles of which three were neutral (two were  $K^0$  and one was a  $\Lambda^0$ ) and 45 were charged (32 positive and 13 negative). Thus  $(24 \pm 5)\%$  of the charged particles were heavy particles. This is in agreement with the results of the Bristol group<sup>26</sup> who found  $25 \pm 8\%$  and Lohrmann and Teucher,<sup>27</sup> who found  $16 \pm 6\%$ . The fraction of particles that are strange particles can only be determined by statistical arguments, since the mass measurements are not sufficiently accurate to distinguish clearly  $K$  particles from protons.

The most straightforward statistical argument is to take the negative heavy particles as strange particles (including negative protons) and assume that on the average in these collisions an equal number of positive particles were created. This would give 26 heavy charged particles *created* in the collisions, or  $(14 \pm 4)\%$  of all charged particles, and leaves 19 positive heavy particles, presumably protons, as participating nucleons. If the total number of heavy particles, taking into account the neutrals, is twice the number of charged heavy particles, and if the total number of pions is 1.5 times the number of charged pions, the fraction of strange particles created compared to the number of pions created would then be  $F = 13 \times 2 \times 2 / 144 \times 1.5$

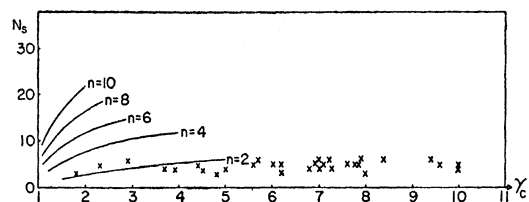


FIG. 12. Estimate of the number of nucleons involved in the collisions. Curves calculated by Ivanovskaya and Chernavsky (reference 23) with experimental results from this experiment.

<sup>26</sup> B. Edwards, J. Losty, D. H. Perkins, K. Pinkau, and J. Reynolds, *Phil. Mag.* **3**, 237 (1958).

<sup>27</sup> E. Lohrmann and M. W. Teucher, *Phys. Rev.* **112**, 589 (1958).

<sup>26</sup> S. Z. Belenky and G. A. Milehin, *Zhur. Exsp. i Teoret. Fiz.* **29**, 20 (1955) [translation: *Soviet Phys.-JETP* **2**, 14 (1956)].

$= (24 \pm 7)\%$ . This number should not be taken too seriously because of the assumptions made in the calculation, but it is of the same order of magnitude as the Heisenberg and Landau predictions. Heisenberg predicts 18% strange particles at 100 Bev and 27% at 1000 Bev. Landau's prediction depends sensitively on the break-down temperature, but for  $m_\pi c^2/kT=1$ , this fraction is 31% and for  $m_\pi c^2/kT=1.5$ , the fraction is 14%.

#### POSITIVE EXCESS AND THE NATURE OF THE PRIMARY PARTICLE

One of the uncertainties of the present experiment is the lack of knowledge of the nature of the incident particle. We have attempted to make inferences on this by consideration of the positive excess of the secondary particles. If all the incident particles were nucleons, the positive excess is expected to be larger than if the incident particles were primarily pions.

Since it was not possible to make accurate identification of the  $K$  mesons, positive and negative, we have calculated the positive excess for all particles observed to emerge from the interaction. Then, taking

$$N^+ = n_p + n_{\pi^+} + n_{K^+} + n_{Y^+}$$

and

$$N^- = n_{\pi^-} + n_{K^-} + n_{\bar{p}} + n_{Y^-},$$

we define P.E.  $= N^+ - N^-$ . Then in a proton-proton collision, for example,  $N^+ - N^- = 2$  and in a  $\pi^- - p$  collision,  $N^+ - N^- = 0$ .

In the case of nucleon-nucleon collisions where cosmic rays at sea level are the source of particles, we take the flux of protons and neutrons to be equal. The expected positive excess if all primaries were nucleons would then be

$$\langle \text{P.E.} \rangle = (2 + 1 + 1 + 0) / 4 = 1.$$

If all the collisions were due to primary pions, the number of interactions produced by positive pions is about 1.3 times<sup>28</sup> the number produced by negative pions, and the positive excess becomes

$$\langle \text{P.E.} \rangle = [2(1.3) + 1(1.3) + 0 + (-1)] / 4.6 = 0.63$$

The observed value is found from  $N^+ = 79_{\pi^+} + 32_{h.p.}$  and  $N^- = 65_{\pi^-} + 13_{H_{h.p.}}$ , in 41 interactions, giving  $\langle \text{P.E.} \rangle = 0.8 \pm 0.2$ .

The value falls between the two predicted values and because of its statistical error, could be compatible with either. It is unlikely, however, that all primaries could be pions, because in 10 cases very energetic protons were found in the forward cone, and these probably correspond to primary nucleons. The observed asymmetry between the forward and backward cone for heavy particles would have been produced if 30%

of the incident particles were pions, and the spectra of nucleons and pions at sea level indicate also that about one-third of the interactions would have been produced by pions.

#### COMPARISON WITH THE FIRE-BALL THEORIES

Models of nucleon-nucleon collisions in which the individual nucleons are excited and radiate separately have been proposed by Kraushaar and Marks,<sup>29</sup> Cocconi,<sup>30</sup> Ciok et al.,<sup>19</sup> Niu,<sup>31</sup> and others. Certain results from photographic emulsions lend support to these theories. We have not made detailed comparison with these theories because of the lack of certainty in angular distributions of *individual* events where the multiplicity is low. Also, in the energy region studied the separation of the secondaries into two cones is not clearly distinguished. The low multiplicities observed in this experiment cast some doubt on the validity of interpretation of highly multiple events, even at higher energies than we have studied, as nucleon-nucleon collisions in which details of the angular distribution are meaningful.

#### SUMMARY AND DISCUSSION

The principal results of the present experiment are as follows:

1. The experimental method used provides more detailed information than has heretofore been available on nuclear reactions in the energy range  $10^{10}$ – $10^{12}$  ev. Further refinements are needed to determine the nature of the primary particle and to improve the statistics.

2. The transverse momentum distribution of the secondary particles gives an average value of  $p_T$  of  $308 \pm 23$  Mev/c.

3. The pions and heavy particles have quite different energy distributions in the c.m. system. The average total energy of the pions is  $420 \pm 40$  Mev and for the heavy particles  $\bar{E}_{(p+K+Y)} = 1262 \pm 194$  Mev.

4. The angular distributions of the pions and heavy particles are different in the c.m. system, with the heavy particles peaking more in the forward and backward direction.

5. The inelasticities found are considerably less than unity, and decrease with increase of energy.

6. The multiplicities observed are quite low in contrast to the multiplicities usually observed in photographic emulsions.

7. About 25% of the particles in these showers may be strange particles (including antinucleons).

We have concluded that in only a small fraction of the events is more than one nucleon of the target involved in a collision, and have made the assumption

<sup>28</sup> G. Puppi and N. Dallaporta, *Progress in Cosmic-Ray Physics*, edited by J. G. Wilson (Interscience Publishers, New York, 1949), Vol. 1, p. 343.

<sup>29</sup> W. L. Kraushaar and L. J. Marks, *Phys. Rev.* **93**, 326 (1954).

<sup>30</sup> G. Cocconi, *Phys. Rev.* **111**, 1699 (1958).

<sup>31</sup> K. Niu, *Nuovo cimento* **10**, 994 (1958).

that the events are nucleon-nucleon collisions for the purposes of the analysis. In the method used for the determination of  $\gamma_c$ , the mass of the primary particle is not an important factor; hence even though some of the collisions may actually be pion-nucleon collisions, the experimental results on angular, energy, and momentum distributions are not dependent on this assumption. The calculations of inelasticity are also practically independent of it.

We have searched without success for a group of interactions with special characteristics which might distinguish them as pion-nucleon collisions instead of nucleon-nucleon collisions. This negative result could mean either that there is no difference between nucleon-nucleon and pion-nucleon collisions at a given energy, that there are very few pions in the cosmic ray beam at these energies, or that the differences were too slight to be obvious in the data we have.

## Numerical Evaluation of the Pion-Nucleon Forward Scattering Amplitude\*

JAMES W. CRONIN

*Palmer Physical Laboratory, Princeton University, Princeton, New Jersey*

(Received July 13, 1959; revised manuscript received January 7, 1960)

The real part of the forward elastic scattering amplitude for  $\pi^\pm$ -proton scattering has been evaluated from experimental cross sections by means of dispersion relations. Recent measurements indicate two peaks in the  $\pi^-$ -proton total cross section at 590 and 870 Mev incident pion kinetic energy. Tables of the real part of the forward scattering amplitude for  $\pi^\pm$ -proton scattering are presented as a function of incident pion kinetic energy in the laboratory. The forward scattering amplitudes obtained from some recent  $\pi^\pm$  scattering experiments are compared with the calculations. Measurement of the forward charge-exchange cross section appears to be the most suitable way of investigating the predictions of the dispersion relation at high energies. The possibility of detecting Coulomb interference at small angles is also discussed.

### I. INTRODUCTION

DISPERSION relations<sup>1-3</sup> have been developed which relate the real part of the forward scattering amplitudes of  $\pi^\pm$ -proton scattering with integrals over the imaginary part of the forward scattering amplitudes. Since the optical theorem relates the imaginary forward amplitude to the total cross section, the real part of the forward amplitude may be calculated from experimentally measured total cross sections. The dispersion relations were used by Sternheimer<sup>4</sup> to calculate the real part of the forward scattering amplitude for  $\pi^\pm$ -proton scattering up to 2 Bev using pion-proton total cross sections measured by Cool et al.<sup>5</sup> More recent calculations by Sternheimer appear in reference 5.

Since the work of Cool et al., extensive measurements have been made of the  $\pi^\pm$ -proton total cross sections. This work was stimulated by the discovery of a resonance in the photoproduction of  $\pi^-$  mesons at a total center-of-mass energy (less proton mass) of 570 Mev.<sup>6</sup>

Burrowes et al.<sup>7</sup> have measured  $\pi^\pm$ -proton total cross sections between 0.5 and 1.2 Bev.<sup>8</sup> Brisson et al.<sup>9</sup> have measured  $\pi^\pm$ -proton cross sections from 0.4 to 1.1 Bev with sharp energy resolution. Devlin et al.<sup>10</sup> have measured  $\pi^\pm$ -proton cross sections from 0.4 to 1.5 Bev. Longo et al.<sup>11</sup> have measured the  $\pi^+$ -proton cross sections from 1.2 to 4.0 Bev. These measurements have revealed two peaks in the  $\pi^-$ -proton cross sections at 590 Mev and 870 Mev instead of a single broad peak found by Cool et al. Figure 1 shows the  $\pi^\pm$ -proton total cross sections based on measurements referred to above.<sup>12</sup> The improved data and new structure warrant a new calculation of the forward scattering amplitudes based on the dispersion relations. Particular attention is given in this paper to applications of the dispersion relations above 300 Mev. Much discussion has been

<sup>7</sup> H. C. Burrowes, D. O. Caldwell, D. H. Frisch, D. A. Hill, D. M. Ritson, R. A. Schluter, and M. A. Wahlig, *Phys. Rev. Letters* **2**, 119 (1959).

<sup>8</sup> All energies unless otherwise specified refer to kinetic energy of the incident pion in the laboratory system.

<sup>9</sup> J. C. Brisson, J. Detoef, P. Falk-Vairant, L. van Rossum, G. Valladas, and L. C. L. Yuan, *Phys. Rev. Letters* **3**, 561 (1959).

<sup>10</sup> T. J. Devlin, B. C. Barish, W. N. Hess, V. Perez-Mendez, and J. Solomon, *Phys. Rev. Letters* **4**, 242 (1960).

<sup>11</sup> M. J. Longo, J. A. Helland, W. N. Hess, B. J. Moyer, and V. Perez-Mendez, *Phys. Rev. Letters* **3**, 569 (1959).

<sup>12</sup> References to the total cross sections below 300 Mev can be found in S. J. Lindenbaum, *Annual Review of Nuclear Science* (Annual Reviews, Inc., Palo Alto, 1957), Vol. 7, p. 317; also in reference 13.

\* This work was supported by the joint program of the Office of Naval Research and the U. S. Atomic Energy Commission.

<sup>1</sup> M. L. Goldberger, *Phys. Rev.* **99**, 979 (1955); R. Karplus and M. A. Ruderman, *Phys. Rev.* **98**, 771 (1955).

<sup>2</sup> M. L. Goldberger, H. Miyazawa, and R. Oehme, *Phys. Rev.* **99**, 986 (1955).

<sup>3</sup> H. L. Anderson, W. C. Davidon, and U. E. Kruse, *Phys. Rev.* **100**, 339 (1955).

<sup>4</sup> R. M. Sternheimer, *Phys. Rev.* **101**, 384 (1956).

<sup>5</sup> R. Cool, O. Piccioni, and D. Clark, *Phys. Rev.* **103**, 1083 (1956).

<sup>6</sup> R. R. Wilson, *Phys. Rev.* **110**, 1212 (1958).